Crystal Structure of Form I of Syndiotactic 1,2-Poly(4-methyl-1,3-pentadiene)

Attilio Immirzi,*,† Consiglia Tedesco,† Stefano Valdo Meille,‡ Antonino Famulari,‡ and Sander van Smaalen§

Dipartimento di Chimica, Università di Salerno, I-84081 Baronissi (SA), Italy, Dipartimento di Chimica del Politecnico di Milano, Milano, I-20121 Italy, and Lehrstuhl für Kristallographie, Universität Bayreuth, D-95440 Bayreuth, Germany

Received October 29, 2002; Revised Manuscript Received March 14, 2003

ABSTRACT: The crystal structure of the form I of syndiotactic 1,2-poly(4-methyl-1,3-pentadiene) has been determined studying the X-ray fiber diffraction pattern recorded onto a Fuji image plate. The chain conformation ($T_6G_2T_2G_2$), previously proposed by Meille et al. on the basis of the identity period, has been confirmed, but with deviations of chain torsion angles from the 60 and 180° values. The crystal system is triclinic, $a = 17.513(8)$ Å, $b = 9.117(6)$ Å, $c = 11.251(14)$ Å, $\alpha = 95.20(4)°$, $\beta = 98.01(3)°$, $\gamma = 92.74(5)°$, and $V = 1768(3)$ Å^3. The space group is $P\bar{1}$, with two chains per cell, each formed by six nonequivalent $CH_2CH[CH{=}C(CH_3)_2]$ chemical units. The crystal structure was determined and refined by the least-squares method, keeping bond lengths fixed and assuming that chemically equivalent bond angles are equal to each other. The refined model shows unrealistic values for some side group bond angles, in particular for the angle between methyl groups. Quite satisfactory results are obtained fixing this angle to the value of 122.7°, as suggested by searching the Cambridge Structural Database. Final disagreement indices are $R_1 = 14.3\%$ and $R_2 = 15.0\%$.

Introduction

Only a few examples of 1,2-syndiotactic polydienes are known: syndiotactic 1,2-poly(butadiene),[1] *cis*-1,2-poly(pentadiene),[2] and 1,2-poly(4-methyl-1,3-pentadiene) (s-P4MPD).[3] The crystal structure has been established only in the first case.[1]

For 4-methyl-1,3-pentadiene, the use of $CpTiCl_3$/MAO (Cp = cyclopentadienyl, MAO = methylallumoxane) as the catalytic system resulted, at low polymerization temperatures, in a syndiotactic polymer (s-P4MPD) with a high molecular weight and high degree of crystallinity. Well-oriented fibers can be obtained by stretching films of the molded material. Samples have as major component a form called I, the object of this study.

The fibrous s-P4MPD exhibits a rather unusual feature: it does not crystallize by adopting one of the usual conformations for syndiotactic vinyl polymers, namely the 2_1 helix,[4] or zigzag planar chain[5] (in such cases the repeating units are all geometrically equivalent); from the observed repeat in fiber diffraction spectra (11.25 Å; ref 3 incorrectly reports the value as $c = 11.73$ Å), a nonregular chain structure is argued. The observed repeat is close to the one observed in the case of form IV of poly(propene), 11.60 Å. To this polymer Chatani[6a] assigned the chain conformation ($T_6G_2T_2G_2$) with six nonequivalent chemical units in the chain crystallographic period. Auriemma et al.[6b] confirmed this chain structure, proposing however a different space group.

By analogy, and also with the aid of conformational analysis, Meille et al.[2] proposed for s-P4MPD the same chain structure. All other chain models gave either high energy or a quite different repeat.

* Corresponding author. E-mail: aimmirzi@unisa.it.
† Università di Salerno.
‡ Dipartimento di Chimica del Politecnico.
§ Universität Bayreuth.

A complete structure determination for s-P4MPD is hindered by the complexity of the crystallographic problem (36 carbon atoms in the asymmetric unit), the difficulty of indexing the fiber spectrum, and the high number of conformational degrees of freedom. On the other hand, the investigation was stimulated by the high crystallinity of the polymer and by the richness of the fiber diffraction pattern with numerous Bragg reflections (Figure 1). The combination of the accurate imaging plate recording technique and the use of a novel computer program especially suited for polymers and based on internal coordinates[7] (see Appendix) made the problem accessible.

Experimental Section

All measurements have been performed on the same fiber sample already used by Meille et. For general chemical information and for the characterization of the polymer with physical methods, see ref 3.

A diffraction pattern was recorded onto Fuji image plates and processed with Fuji-Bas 2500 image plate reader. The pixel size was set to 50 μm × 50 μm.

Measurements were performed using (i) a flat-film geometry and Mo Kα radiation with a sample to film distance of 100 mm and (ii) a cylindrical camera of 57.30 mm radius under vacuum with graphite-monochromated Cr Kα radiation.

We have used in this work only the second data set because it gives the better resolution, albeit diffracted intesities are measurable only for $l \leq 2$. The Mo Kα data set (which could afford improvement in atomic positions since l ranges from 0 up to 6) has revealed itself very difficult to process because of the frequent occurrence of overlap of Bragg reflections. While 49 intensity data were obtained from the Cr spectrum (of which 26 are single Bragg reflections), 54 intesity data were drawn from Mo spectrum, but only 14 are not overlapped (see Figure 1).

Results and Discussion

Unit Cell and Space Group Determination. The fiber diffraction pattern of form I of s-P4MPD as

10.1021/ma0257853 CCC: $25.00
Published on Web 04/24/2003

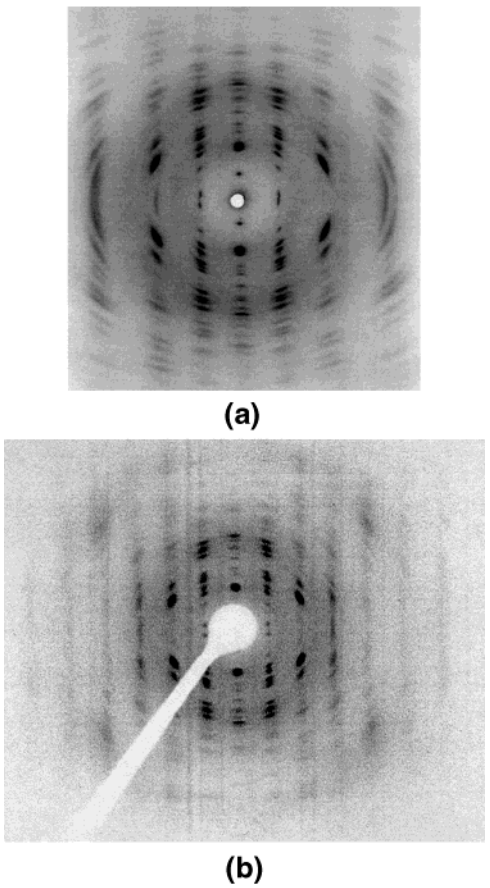

Figure 1. Fiber diffraction pattern of s-P4MPD recorded by a Fuji image plate: (a) Cr Kα radiation, cylindrical camera under vacuum, radius 57.30 mm; (b) Mo Kα radiation, flat plate, sample distance 100 mm.

recorded with Cr Kα radiation is shown in Figure 1. Almost 150 reflections, distributed over 4 quadrants and with $|l| = 0-3$, are visible. Their positions were used for indexing with the aid of an interactive computer program. One obtains a triclinic unit cell with lattice constants $a = 17.513(8)$ Å, $b = 9.117(6)$ Å, $c = 11.251(14)$ Å, $\alpha = 95.20(4)°$, $\beta = 98.01(3)°$, $\gamma = 92.74(5)°$, and $V = 1768(3)$ Å^3 (values obtained by least-squares fitting of the IP coordinates). By using the LePage program devised by Spek,[8] it has been ascertained that the lattice is truly triclinic and unit cells of higher symmetry do not exist. The experimental density (0.91 g/cm^3) is well reproduced if the cell contains two six-unit chains (0.92 g/cm^3). This suggested the hypothesis that the space group is $P\bar{1}$, with the asymmetric unit consisting of a single six-unit chain. This hypothesis was confirmed by the structure analysis and refinement. Because the polymer is conformationally chiral, the $P\bar{1}$ crystal contains equal amounts of chains of opposite chirality.

The alternative $P1$ (which cannot be excluded on a logical basis) was not pursued since it appears very unrealistic: the cell should contain two chains, crystallographically nonequivalent but parallel to each other and with the same repeat (and reasonably the same conformation, see later) either of the same conformational chirality or of opposite chirality. In the former case, a halved unit-cell volume should have been observed; in the latter case this strange $P1$ structure should be a distortion of the $P\bar{1}$ structure.

Integrated Intensity Evaluation. To obtain the integrated intensities and the experimental structure factors only one quadrant of the spectrum has been considered with l limited to 2. The software implemented by Raytest[9] was not used, since it allows only the surface integrals of the PSL values to be computed with the difficulty that the background level must be chosen by the user peak-by-peak (and rather arbitrarily). The difficulties for weak and/or quasi-overlapped reflections are evident.

Furthermore, although we obtained in the past good results using just surface integrals,[10−12] the frequent reflection overlap suggested to prefer the method by Cella et al.[13] who assert that, in the case of fiber spectra, the correct structure factors must be computed by linear integration along increasing ϑ lines and applying appropriate correction factors to these integrals.

For this purpose a new program has been devised for obtaining integrated intensities from IP images.[14] This homemade software, still under implementation, allows treating both cylindrical-film and flat-film IP images (also with the plate nonorthogonal to the incident beam). It allows first to setup the background line with a quasi-automated procedure and then to perform surface integrals as well as two different types of line integrals: along constant ϑ lines and along increasing ϑ lines. The latter integrals were used to determine integrated intensity for isolated reflections; the former type of line integrals were used, as complementary information, in the case of partially overlapped reflections (e.g., the strong equatorial reflections 2 0 0, $\bar{1}$ 1 0, and 1 1 0 in Table 1).

The data were corrected for polarization and Lorentz factors, and corrected according to Cella et al.[13] to be used in further analysis.

The Isolated Chain. The 31 internal coordinates (IC) used for describing the chain and crystal structures are indicated in Figure 2 and Table 2.

Also using internal coordinates, the number of degrees of freedom of the structural model remains high. Thus, we performed a preliminary conformational analysis to estimate the orientation for the six side groups. A backbone ($T_6G_2T_2G_2$) conformation with standard torsion angles, i.e., 60 and 180°, has been assumed. It is worth noting that this backbone conformation has C_2 molecular symmetry. Since full computation of a 6-dimensional energy map is prohibitive, we have considered 2−3 variables in turn and concluded last that also the side group conformation roughly obeys C_2 symmetry; in the absolute energy minimum $\vartheta_{13} \approx \vartheta_{18}$, $\vartheta_{14} \approx \vartheta_{17}$, and $\vartheta_{15} \approx \vartheta_{16}$.

The chain potential energy was computed using the potential function by Halgren[15] considering, for simplicity, only the van der Waals contributions. At the end we concluded that there is unique low-energy combination of side-group conformations, viz. the one with $\vartheta_{13} = 264°$, $\vartheta_{14} = 144°$, and $\vartheta_{15} = 239°$. These side group conformations were used in the starting model for the crystal structure analysis.

As the internal energy of the chain (∼94 kcal per monomeric unit) is substantially higher than the packing energy (∼4 kcal per monomeric unit), the C_2 symmetry of the isolated chain could be maintained in the crystal although the triclinic symmetry allows for distortions of the chains. The large chain potential energy is certainly due to the bulky side groups.

Structure Determination. The structure was solved by a direct-space search method, assisted by the novel

Table 1. Observed and Calculated Squared Structure Factors[a]

h	*k*	*l*	*	F_o^2	F_c^2(A)	F_c^2(B)	F_c^2(C)	F_c^2(D)	y_o	y_c	*h*	*k*	*l*	*	F_o^2	F_c^2(A)	F_c^2(B)	F_c^2(C)	F_c^2(D)	y_o	y_c
1	0	0		87	185	33	274	106	7.51	7.49	−3	−2	1		349	20	102	0	90	36.92	36.52
2	0	0		759	702	793	621	701	15.06	15.01	−5	0	1	o		2	27	1	155		36.75
−1	1	0		826	819	828	806	807	15.76	15.78	4	1	1	o		199	136	250	112		36.95
1	1	0		971	1096	1011	1016	894	16.56	16.60	−5	1	1		341	394	330	391	533	39.26	39.24
−2	1	0		120	36	140	25	97	20.20	20.16	5	0	1		257	39	24	47	186	40.63	40.37
2	1	0		53	32	30	154	193	21.51	21.45	3	2	1	o		20	40	48	42		40.58
3	0	0		190	3	108	82	152	22.56	22.60	4	−2	1	u		20	147	26	10		41.97
−3	1	0		276	276	248	253	296	26.16	26.10	−6	0	1	u		49	133	58	10		44.84
3	1	0		39	1	15	23	5	27.66	27.62	−1	3	1		268	109	173	48	113	45.32	45.65
−1	2	0		193	208	253	131	175	29.65	29.44	2	−3	1	o		3	46	0	1		45.74
4	0	0		462	5	218	9	14	30.35	30.30	0	3	1	o		10	0	144	0		45.76
1	2	0	o		389	230	451	570		30.36	1	3	1	u		196	106	200	42		47.24
−4	1	0		508	531	373	576	577	32.75	32.83	6	−1	1	u		31	162	29	38		49.66
4	1	0		1275	1202	1126	11 166	1089	34.61	34.49	−3	−3	1		58	58	32	55	1	50.07	49.97
−3	2	0		197	221	233	183	254	35.76	35.85	2	3	1	o		116	86	182	177		50.02
5	0	0		148	73	12	45	84	37.91	38.14	−4	−3	1		79	20	0	17	18	54.72	54.57
3	2	0	o		6	49	0	107		38.14	−7	1	1	o		32	76	113	143		54.79
−4	2	0		105	92	59	88	128	40.90	41.00	−8	1	1	u		30	169	55	70		63.18
4	2	0		320	26	109	13	127	44.12	43.73	0	0	2	m		59	16	69	0		0.00
0	3	0	o		140	183	54	123		43.99	−1	0	2	m		319	1	99	88		0.00
−1	3	0	o		2	4	2	26		44.20	−2	0	2		3142	1702	1803	11 792	1908	11.38	11.23
−6	2	0	u		8	100	58	109		53.74	1	0	2	o		1444	1345	11 353	1197		10.39
0	0	1		10	18	7	23	61	1.76	1.61	0	−1	2	u		1	161	24	208		11.97
−1	0	1	u		19	275	8	45		5.83	−1	1	2		837	15	2	0	114	16.64	16.74
1	0	1		67	74	0	94	113	9.47	9.26	0	1	2	o		830	764	613	640		17.00
0	−1	1		473	335	335	370	375	13.57	13.36	−2	−1	2		318	184	174	191	334	17.30	17.57
−2	0	1	o		217	201	272	237		13.44	−3	0	2	u		279	315	100	62		19.51
−1	−1	1	u		32	143	94	231		14.96	1	1	2	u		12	152	48	117		20.55
0	1	1		588	649	563	580	493	15.62	15.70	2	−1	2	u		19	149	8	7		21.82
1	−1	1	o		4	55	7	73		15.78	−3	−1	2		81	1	33	33	13	24.48	24.10
2	0	1		104	28	7	0	10	16.72	16.89	0	−2	2		112	3	70	26	5	27.39	27.51
1	1	1		502	605	576	592	588	18.67	18.56	−4	0	2	o		41	7	0	7			27.68
−2	−1	1		634	46	8	70	19	19.87	19.64	−1	−2	2	u		162	443	29	451			28.16
−2	1	1	o		606	657	619	736		19.99	3	−1	2		389	390	327	259	350	29.04	28.91
2	−1	1	u		99	137	60	130		20.89	1	−2	2	o		0	24	1	3			29.13
−3	0	1		596	479	618	571	683	21.21	21.10	−2	−2	2	u		309	591	182	237			30.95
2	1	1		77	223	79	274	205	23.67	23.67	−1	2	2		605	177	92	230	369	32.27	32.17
−3	1	1		106	128	43	186	86	25.72	25.56	0	2	2	o		267	345	264	176			32.54
−3	−1	1	o		7	146	26	54		25.83	−3	−2	2		127	1	5	7	3	35.63	35.42
3	−1	1		1169	1187	1177	11 116	1102	27.57	27.28	−5	0	2	o		3	14	29	18			35.92
1	−2	1		1178	840	1055	11 017	1008	29.51	29.07	−4	2	2		105	169	264	232	221	41.98	41.88
−1	−2	1	o		421	232	260	203		29.11	1	−3	2		110	13	54	2	8	44.43	44.28
0	2	1		1286	335	615	161	158	30.47	30.44	−6	0	2	o		29	6	23	3			44.34
−1	2	1	o		722	639	921	1137		30.52	5	−1	2	o		58	7	7	0			44.51
2	−2	1	u		40	120	37	27		32.01	−5	−2	2		186	0	11	11	46	47.88	47.69
−2	−2	1		1682	541	568	586	570	32.52	32.07	−5	2	2	o		130	189	239	175			47.69
−4	1	1	o		261	417	154	516		32.11	5	1	2	o		49	16	69	28			47.99
4	0	1	o		29	86	24	0		32.40	−1	3	2	o		1	1	21	13			48.17
1	2	1	o		235	221	188	83		32.29	4	2	2		168	2	45	10	0	50.39	50.07
−2	2	1	o		290	82	538	155		32.51	3	−3	2	o		55	24	12	5		50.41
−4	−1	1	o		380	344	292	326		32.76	1	3	2	o		72	85	124	181		50.44
4	−1	1	u		92	142	57	202		34.33	−7	2	2	u		419	268	277	456		61.73
−3	2	1	u		57	126	0	50		36.13	0	4	2	u		372	156	509	661		65.76

[a] The $F^2(hkl)$ are ordered by increasing 2ϑ angle within each layer, and are normalized to the scattering of a unit-cell with a multiplying factor 0.050. Hydrogen atom contributions were included and isotropic thermal parameter was set to $B = 2.0, 8.0, 2.0, 3.0$ Å^2 in A, B, C, and D cases, respectively. Reflections marked with "m" (meridional) are visible but not measurable. Unobserved reflections, marked with "u", are included only if F_c^2 is greater than 100. Reflections overlapped with the preceding one are marked with "o" and F_o^2 must be compared with the sum of overlapping F_c^2. y_o and y_c are, respectively, the observed and calculated vertical positions of peaks on the IP (mm).

interactive program TRY developed by one of us[7] and fully based on internal coordinates. As summarized in the Appendix, TRY allows model building (using both diffraction data and potential energy) and structure refinement (using only diffraction data).

The structural model was constructed assuming that (i) the chemically equivalent bond-lengths are equal and known, (ii) the chemically equivalent bond angles are equal but unknown; (iii) the torsion angles are distinct and unknown, and (iv) the ethylenic moiety in the side group is strictly planar.

In the early stages of the analysis, the C_2 symmetrical chain was considered as a rigid body (including side group torsion angles set up to the values obtained from the conformational analysis) with the chain axis parallel to the crystallographic *c* axis. Making systematic translations and rotations about the chain axis (four variables altogether), and computing step-by-step the packing energy, one obtains a number of plausible models. At this stage coarse increments of the parameters were sufficient, since TRY performs, step-by-step, also a steepest-descent local adjustment of the variables. Evaluation of the structure factors and comparison with the experimental ones gave only one plausible hypothesis corresponding to a good low-energy packing and an acceptable reliability factor (∼34−40%) based on $F^2(hkl)$.

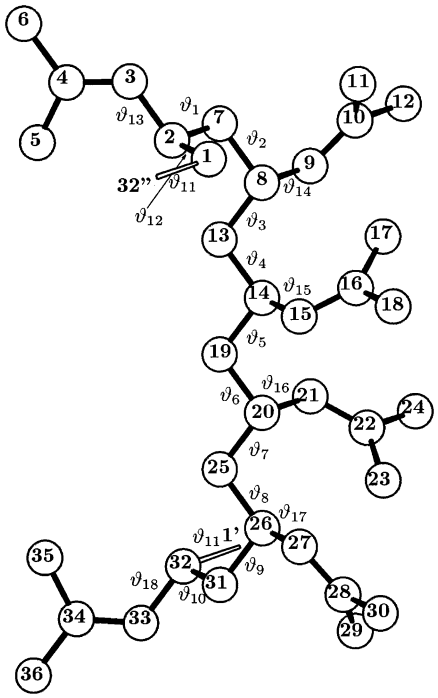

Figure 2. Schematic model of the ($T_6G_2T_2G_2$) chain of s-P4MPD (H atoms omitted). The chain segment represents the crystallographic asymmetric unit. The atom numbering and the definition of the torsion angles ϑ_i (i = 1−16) is indicated. Chain conformations are set to 180 (T) and 60° (G). The model is oriented so that the chain 2-fold axis crossing C19 atom is horizontal.

Optimization of Crystalline Structure. The program TRY allows to perform both structure "adjustment" using a steepest-descent procedure (either pursuing the lowest packing energy or the lowest R_2 disagreement index) and structure "refinement" based on the multivariate least-squares fitting of the diffraction data. In the latter case the F_o^2 values, obtained from the IP, are compared with the corresponding F_c^2, considering the sum of F_c^2 in the case of overlap. More exactly F_c^2 values are summed when the calculated y coordinates of the reflections on the IP differ less than 0.5 mm (see Table 1; an exception have been made for the 1 0 2 and −2 0 2 reflections. The sum of F^2_c was used although the separation is 0.83 mm, since −2 0 2 is very strong and it is extended ∼5 mm). Least-squares refinements have been made both for the C_2 symmetrical chain model and for the unsymmetrical C_1 chain model.

In the case of polymers, one must take care that structural changes fulfil, step by step, the chain continuity.[16] In absence of chain symmetry for a chain with N_B backbone atoms, with given bond-angles and given chain repeat, the number of conformational degrees of freedom is $N_B - 4$. The structure refinement consists of finding (using for instance the Lagrange method) the minimum value of a N_V variable function to which N_C constraints are imposed, being $N_V - N_C = N_B - 4$. Several choices are possible, but it is practical to use as few constraints as possible in order to prevent ill-conditioned matrices and reduce matrix size (the order of matrices is $N_V + N_C$). In the case of nonhelicized chains without symmetry, it is practical to consider $N_B - 2$ torsion angles and 2 constraints. Of course the unused torsion angles are well determined provided that continuity is strictly obeyed.

The adopted procedure for the unsymmetric C_1 case is the following: the backbone atoms C1, C2, ..., C32 are built-up using the nine torsion angles $\vartheta_1...\vartheta_9$, and C32″ atom is defined using the torsion angles ϑ_{12} (the ′ operator designates the forward repetition, ″ the backward). The vector C32″−C1 is then translated onto C32 obtaining C1′ with a C31−C32−C1′ bond angle possibly different from τ_2. The constraints to be applied are that the bond angle C31−C32−C1′ is equal to τ_2 and that the C1−C1′ distance is equal to the fiber repeat c. Besides 10 torsion angles other parameters to be considered are as follows: two chain bond angles τ_1,τ_2, six side torsion angles $\vartheta_{13}...\vartheta_{18}$, three side bond angles τ_3, τ_4, τ_5, and four parameters Φ, x_0, y_0, z_0 defining the orientation and position of the molecule. One obtains 25 variables altogether (model B, Table 2).

In the case of C_2 molecular symmetry the following relations exist between parameters: $\vartheta_i = \vartheta_{11-i}$ for i = 6−10 and $\vartheta_i = \vartheta_{31-i}$ for i = 16−18. A slightly different procedure has been adopted: five torsion angles $\vartheta_1...\vartheta_5$ are used for building the sequence of atoms C1...C1′; the C1′−C32 vector is translated onto C1 to set the C32″ atom; two constraints are used C32″−C1−C2 = τ_1 and C1−C1′ distance = fiber repeat c. The number of variables is reduced to 15 (model A, Table 2).

Besides models A and B, two other models (C and D) were tested, as they were suggested by the unsatisfactory side-group geometry obtained in the refinement of models A and B (see later). Models C and D differ from A and B for having τ_5 angle fixed to 122.7°; this figure is the average value observed for single-crystal structures classified in the Cambridge Structural Database and containing the above fragment.[17]

All refinements were done by releasing the backbone parameters first and then releasing the other parameters, finally performing a "full-matrix" refinement. After some oscillations convergence was obtained in all cases to the values reported in Table 2. Resulting R indices and shortest packing distances are reported in Table 3.

R indices seem to indicate that model B gives a better fit to the data than model A. This was confirmed by Hamilton's test,[18] the ratio $R_2(A)/R_2(B)$ = 1.403 is greater than 1.309 as calculated for a significance level of 0.05. The better packing distances found in model B strengthen this conclusion.

For both models A and B (see Table 2), while the resulting geometry of the backbone is credible (the τ_1 bond angle is however rather small), the side-group bond angles τ_3, τ_4, and τ_5 are unrealistic. These deficiencies concern peripheral regions of the macromolecule and they might be a consequence of some conformational disorder.[19] As appears in Table 3, the R indices in cases C and D exceed those for A and B only moderately. Furthermore, the refined bond angles are positively better and the indication that the packing is better without C_2 chain symmetry is confirmed. On the whole D model, despite the sligthly higher R indices, decidedly represents the most satisfactory result. Table 4 lists the atomic fractional coordinates for case D only.

The cross examination of the 49 observed intensities and the corresponding calculated ones (see Table 1) shows acceptable discrepancies. Also 188 unobserved hkl were computed (in Table 1 only the most critical ones are given); none of them is particularly high.

Crystal Packing. The packing of s-P4MPD (see Figure 3) displays a substantial difference with respect

Table 2. Internal Coordinates for s-P4MPD as Resulted at the End of the Structure Refinements A, B, C, and D ($A = C_2$ Model, B = C_1 Model, C, D = as A, B with Fixed Geometry in Ethylenic Moiety)[a]

		A	B	C	D
b_1	C−C bond length in chain	*1.540*	*1.540*	*1.540*	*1.540*
b_2	C−C bond length in side group	*1.540*	*1.540*	*1.540*	*1.540*
b_3	C=C bond length in side group	*1.340*	*1.340*	*1.340*	*1.340*
b_4	C−H bond length	*1.080*	*1.080*	*1.080*	*1.080*
τ_1	C−C−C bond angle (chain, on CH_2)	103.9(14)	104.0(15)	109.1(15)	111.5(11)
τ_2	C−C−C bond angle (chain, on CH)	102.7(11)	106.5(12)	105.7(10)	107.1(8)
τ_3	C−C−C bond angle (side, sp^3)	97.5(20)	101.8(16)	101.9(18)	106.5(12)
τ_4	C−C=C bond angle (side, sp^2)	116(3)	119(3)	118(3)	121(2)
τ_5	C=C−C bond angle (side, sp^2)	138(2)	141(3)	*122.7*	*122.7*
τ_6	CH_3 −C−CH_3 (=360 − $2\tau_5$)	83.4	78.8	*114.6*	*114.6*
ϑ_1	torsion angle (about C2−C7)	−66(4)	−64(6)	−56(4)	−66(4)
ϑ_2	torsion angle (about C7−C8)	−71.1(20)	−73(4)	−71.4(3)	−44.4(4)
ϑ_3	torsion angle (about C8−C13)	198(4)	199(6)	188(4)	181(6)
ϑ_4	torsion angle (about C13−C14)	195(7)	193(6)	190(7)	177(7)
ϑ_5	torsion angle (about C14−C19)	166(3)	176(7)	177(3)	178(8)
ϑ_6	torsion angle (about C19−C20)	$=\vartheta_5$	187(6)	$=\vartheta_5$	185(7)
ϑ_7	torsion angle (about C20−C25)	$=\vartheta_4$	197(7)	$=\vartheta_4$	200(6)
ϑ_8	torsion angle (about C25−C26)	$=\vartheta_3$	159(7)	$=\vartheta_3$	183(5)
ϑ_9	torsion angle (about C26−C31)	$=\vartheta_2$	−73(6)	$=\vartheta_2$	−97(3)
ϑ_{10}	torsion angle (about C31−C32)	$=\vartheta_1$	−74.1*	$=\vartheta_1$	−47.1*
ϑ_{11}	torsion angle (about C32−C1′)	−172.0*	−156.6*	−177.0*	−170.5*
ϑ_{12}	torsion angle (about C1−C2)	−172.0*	181(6)	−177.0*	−194(4)
ϑ_{13}	torsion angle C7−C2−C3−C4	249(3)	252(5)	251(3)	256(5)
ϑ_{14}	torsion angle C13−C8−C9−C10	177(6)	190(8)	159(6)	162(6)
ϑ_{15}	torsion angle C19−C14−C15−C16	202(4)	201(5)	216(40)	208(7)
ϑ_{16}	torsion angle C19−C20−C21−C22	$=\vartheta_{15}$	215(7)	$=\vartheta_{15}$	221(6)
ϑ_{17}	torsion angle C25−C26−C27−C28	$=\vartheta_{14}$	181(6)	$=\vartheta_{14}$	169(7)
ϑ_{18}	torsion angle C31−C32−C33−C34	$=\vartheta_{13}$	259(5)	$=\vartheta_{13}$	265(5)
Φ	chain rotation about *z*	293.0(10)	296(3)	292.4(11)	284.5(19)
x_0	chain translation along *x*	5.34(9)	4.96(11)	5.56(9)	5.38(8)
y_0	chain translation along *y*	2.48(6)	2.31(10)	2.61(5)	2.80(8)
z_0	chain translation along *z*	7.38(6)	7.25(9)	7.27(7)	7.37(9)

[a] Bond lengths and translations are in Å, angles are in deg. Values in italics were kept constant. In A and C cases several quantities are equal in pairs as indicated. Standard uncertainities (in parentheses) were computed from the normal matrix in the final full-matrix least-squares refinement cycle. For atom labeling and the definition of the principal torsion angles see also Figure 2. Overall rotation of the chain (Φ) is defined as the dihedral angle of *x*, *z* crystallographic plane with the C1−C19−C7 plane. Overall translations (x_0, y_0, z_0) are referred to the C19 atom. Chain torsion angles marked with an asterisk are calculated from other chain torsion angles.

Table 3. Disagreement Indices and Short Interatomic Packing Distances for s-P4MPD for A, B, C, and D Least-Squares Refinements[a]

	symm.	N_V	df	R_1	R_2	packing distances (Å)
A	C_2	17	15	0.143	0.156	2.84, 3.45, 3.67, 3.68
B	C_1	25	23	0.115	0.123	3.17, 3.41, 3.54, 3.66
C	C_2	15	13	0.171	0.196	2.65, 3.16, 3.47, 3.68
D	C_1	23	21	0.134	0.148	3.37, 3.39, 3.44, 3.46

[a] In A and C cases the C_2 chain symmetry was considered; in C and D cases two bond angles were held fixed; df is the number of degrees of freedom.

Table 4. Fractional Coordinates of the Carbon Atoms of s-P4MPD for D Model (C_1 Chain Symmetry)

atom	*x/a*	*y/b*	*z/c*	atom	*x/a*	*y/b*	*z/c*
C1	0.3199	0.3094	1.2242	C19	0.2938	0.2805	0.7396
C2	0.3826	0.2191	1.1743	C20	0.2388	0.3034	0.6244
C3	0.4440	0.1994	1.2828	C21	0.2286	0.1543	0.5461
C4	0.5194	0.2047	1.2725	C22	0.1595	0.1043	0.4859
C5	0.5498	0.2304	1.1536	C23	0.0863	0.1905	0.4903
C6	0.5826	0.1856	1.3787	C24	0.1469	−0.0441	0.4066
C7	0.3452	0.0643	1.1287	C25	0.2815	0.4116	0.5551
C8	0.2814	0.0697	1.0203	C26	0.2459	0.4018	0.4213
C9	0.2714	−0.0862	0.9528	C27	0.1628	0.4509	0.4185
C10	0.2265	−0.1925	0.9878	C28	0.1123	0.4325	0.3165
C11	0.1824	−0.1673	1.0963	C29	0.1331	0.3622	0.1965
C12	0.2150	−0.3497	0.9228	C30	0.0287	0.4800	0.3099
C13	0.3133	0.1723	0.9349	C31	0.2902	0.5190	0.3626
C14	0.2544	0.1835	0.8214	C32	0.3550	0.4518	0.3000
C15	0.1880	0.2704	0.8630	C33	0.3757	0.5601	0.2103
C16	0.1250	0.2007	0.8917	C34	0.4340	0.6631	0.2410
C17	0.1143	0.0314	0.8853	C35	0.4838	0.6808	0.3661
C18	0.0574	0.2835	0.9336	C36	0.4565	0.7735	0.1540

to the packing of the other known syndiotactic polymer with ($T_6G_2T_2G_2$) chain conformation, viz. form IV of syndiotactic poly(propene).[6] While crystalline s-P4MPD contains equal amounts of chains of opposite chirality (in conformational sense!), form IV of syndiotactic poly(propene), claimed to be $P1$[6a] or $C2$,[6b] contains chains of a unique chirality. The same occurs also in the case of the β'' form of syndiotactic poly(styrene) (TGGT conformation) which is $P2_12_12_1$.[20]

In more detail, in s-P4MPD each chain is surrounded by six chains, two isochiral and four antichiral, with a roughly hexagonal disposition. Furthermore, the shortest intermolecular interactions between side groups take place between antichiral chains.

It is also worthwhile to compare s-P4MPD with its "saturated" analogue, namely the syndiotactic poly(4-methyl-1-pentene)(s-P4MP),[21] which crystallizes in the tetragonal system forming a 12/7 helix (12 pairs of monomers in 7 turns). The volume per monomeric unit in the crystalline state (unit-cell volume divided by the number of monomers per cell) are 158.8 Å^3 for s-P4MP and 147.3 Å^3 for s-P4MPD; the difference of 11.5 Å^3 should represent the solid-state volume of two H atoms. The observed value is about two times larger than the values derived from the experimental densities of pairs of small molecules, as butyrric acid ($C_4H_7O_2$) and crotonic acid ($C_4H_5O_2$), ∼5 Å.[3] This indicates that s-P4MPD is more tightly packed than s-P4MP. The comparison of melting temperatures, ∼100 °C for s-P4MPD and 210 °C for s-P4MP, indicates that the solid-state entropy is considerably increased by the saturation. The richness of s-P4MPD fiber pattern as

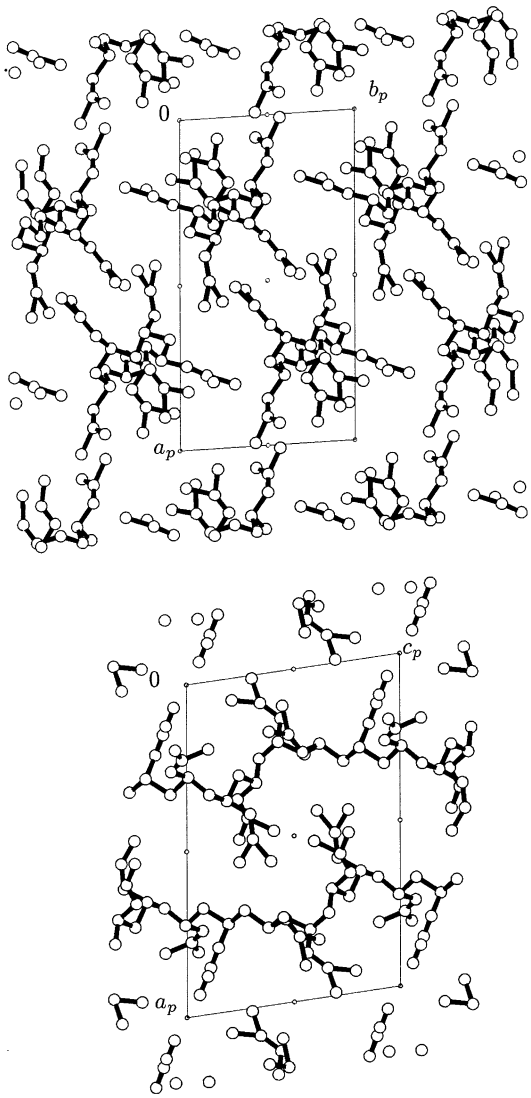

Figure 3. Crystal packing of s-P4MPD as results for model B projected along *c* edge (up) and along *b* edge (down). H atoms are omitted.

compared to the few reflections observed for s-P4MP is indicative of a high degree of disorder and is coherent with this observation.

Conclusions

The elucidation of the structure of syndiotactic 1,2-poly(4-methyl-1,3-pentadiene) has contributed to a better understanding of the unusual chain conformation $T_6G_2T_2G_2$, already observed in syndiotactic poly(propene) but not in vinyl polymers with bulky (and unsaturated) side groups.

In our opinion, the main result of the present work is that it has shown that the crystalline polymer structure can be determined by a rigorous least-squares refinement, using few parameters. The systematic use of the internal coordinates has played a crucial role, as well as the accuracy of the diffraction measurements (image-plate-detector technique). The use of a dedicated computer program with many options specific for polymers, including the ones for imposing chain continuity constraints, also played an important role.

Acknowledgment. This work has been supported by the Consiglio Nazionale delle Ricerche and by the Ministero dell'Istruzione Universitaria e della Ricerca (local projects and PRIN 1999−2001).

Appendix

TRY is an interactive computer program, particularly suited for polymers, useful in crystal structure analysis from diffraction data. TRY is practical in handling difficult problems with many variables and few data, and it is applicable both in the early stages of the analysis and in the refinement stages.

TRY does not use atomic coordinates but internal parameters (bond lengths, bond angles, torsion angles, overall rotations and translations, etc.). Structures are set up through a sequence of symbolic "building commands" according to a language similar to the one devised in another program.[22] Each command performs a given operation acting on specified atoms and parameters. For example the command

setx C1 C7 O3 C6 g1 g3 g7

creates the atom labeled C6 at a distance g1 from O3 with a bond angle C7−O3−C6 equal to g3 and a torsion angle C1−C7−O3−C6 of g7.

In the early stages of the analysis internal parameters can be modified either by trial and error or by systematic searches in the parameter space driven by computing structure factors, and/or packing energy. Step-by-step the packing diagram can be displayed on the screen and the conventional disagreement indices calculated ($j = h, k, l$):

$$R_1 = \frac{\sum_j [|F_{j,\mathrm{obs}}| - |F_{j,\mathrm{calc}}|]^2}{\sum_j |F_{j,\mathrm{obs}}|} \qquad R_2 = \frac{\sum_j [F_{j,\mathrm{obs}}{}^2 - F_{j,\mathrm{calc}}{}^2]^2}{\sum_j F_{j,\mathrm{obs}}{}^2}$$

Furthermore, there is the possibility of "monitoring" the influence of the individual parameters on packing and lattice energy. Convergence of the parameter-space search procedure is improved by the steepest-descent method either pursuing the lowest R_2 index or the lowest packing energy. In any case parameters and not atomic coordinates are modified. For the evaluation of the R values the scale factor is optimized in each cycle as the value which minimizes R_2. Average (isotropic) thermal parameters are tested, and their variation is proposed; the user can decide whether to apply it or not.

In the refinement stages TRY uses the least-squares method selected internal parameters, without restraints among them. The minimized quantity is the above R_2 index. Excluding bond lengths from the list of refined parameters allows a bond-constrained refinement; excluding bond-angles allows angle-constrained refinement. Highly torsionally flexible structures can be refined releasing only partially the torsion angles. By simply using the same symbol for several variables one imposes the equality of the given parameters.

For the case of polymers special commands have been implemented for generating regular helices. Furthermore, to ensure the *chain continuity*,[16] least-squares refinement is carried out reducing the number of degrees of freedom for the backbone atoms and using the method of Lagrange multipliers. The above "symbolic language" is also used for defining the Lagrange constraints, provided they can be expressed as a simple function of distances, angles, etc.

TRY includes a large choice of options (including the powder profile refinement according to Rietveld) not all

fully tested. For these reasons it has been not yet published and distributed. The author will be pleased in establishing collaborations with other potential users (especially polymer crystallographers) for further testing and improvements.

Note Added after ASAP Posting

This article was released ASAP on 4/24/2003. In Table 2, column 1, σ was changed to Φ, and in Table 3, NV was changed to N_V in the heading for column 3. The correct version was posted on 5/5/2003.

References and Notes

(1) (a) Natta, G.; Corradini, P. *Rend. Acc. Naz. Lincei Ser. 8* **1955**, *19*, 229. (b) Natta, G.; Corradini, P. *J. Polym. Sci.* **1956**, *20*, 251.

(2) Ricci, G.; Italia, S.; Porri, L. *Macromolecules* **1994**, *27*, 868.

(3) Meille, S. V.; Capelli, S. *Macromol. Rapid Commun.* **1995**, *16*, 891.

(4) (a) Corradini, P.; Natta, G.; Ganis, P.; Temussi, P. A. *J. Polym. Sci., Part C: Polym. Lett.* **1967**, *16*, 2177. (b) Chatani, Y.; Shimane, Y.; Inagaki, T.; Ijitsu, T.; Yukinari, T.; Shikuma, H. *Polymer* **1993**, *34*, 1620.

(5) (a) Chatani, Y.; Maruyama, H.; Noguchi, K.; Asanuma, T.; Shiomura, T. *J. Polym. Sci., Part C: Polym. Lett.* **1990**, *28*, 393. (b) De Rosa, C.; Guerra, G.; Petraccone, V.; Corradini, P.. J. *Polym. J. (Tokyo)* **1991**, *23*, 1435.

(6) (a) Chatani, Y.; Maruyama, H.; Asanuma, T.; Shiomura, T. *J. Polym. Sci., Part B: Polym. Phys.* **1991**, *29*, 1649. (b) Auriemma, F.; De Rosa, C.; Ruiz de Ballesteros, O.; Vinti, V.; Corradini, P. *J. Polym. Sci., B* **1998**, *36*, 395.

(7) Immirzi, A. Unpublished work.

(8) Spek, A. L. *J. Appl. Crystallogr.* **1988**, *21*, 578.

(9) AIDA software, Raytest GMBH, Straubenhardt, Germany.

(10) Oliva, L.; Immirzi, A.; Tedesco, C.; Proto, A. *Macromolecules* **1999**, *32*, 2675.

(11) Immirzi, A.; Tedesco, C.; Venditto, V.; Recupero, D.; van Smaalen, S. *Macromolecules* **2000**, *33*, 125.

(12) Antinucci, S.; Monaco, G.; Immirzi, A. *Macromolecules* **2001**, *34*, 8078.

(13) Cella, R. J.; Lee, Byungkook; Hughes, R. E. *Acta Crystallogr.* **1970**, *A26*, 118.

(14) Immirzi, A. Unpublished work.

(15) Halgren, T. A. *J. Comput. Chem.* **1996**, *17*, 490−641 (several articles describing the Merck Molecular Force Field MMFF94).

(16) Tadokoro, H. *Structure of Crystalline Polymers*; J. Wiley & Sons: New York, 1979; p 136.

(17) Bruno, I. J.; Cole, J. C.; Edgington, P. R.; Kessler, M.; Macrae, C. F.; McCabe, P.; Pearson, G.; Taylor, R. *Acta Crystallogr.* **2002**, *58*, 389−397.

(18) Hamilton, W. C. *Acta Crystallogr.* **1965**, *18*, 502.

(19) Stout, G. H.; Jensen, L. H. *X-ray Structure Determination*, 2nd ed.; Wiley-Interscience: New York; p 397.

(20) De Rosa, C.; Rapacciuolo, M.; Guerra, G.; Petraccone, V.; Corradini, P. *Polymers* **1982**, *33*, 1423.

(21) De Rosa, C.; Venditto, V.; Guerra, G.; Corradini, P. *Macromolecules* **1992**, *25*, 6398.

(22) Immirzi, A.; Brückner, S. *J. Appl. Crystallogr.* **1997**, 207.

MA0257853